Partial Pair Correlation Functions of Highly Concentrated Aqueous Urea Solutions Determined by Neutron Diffraction with $^{14}N/^{15}N$ and H/D Isotopic Substitution Methods

Yasuo Kameda,* Asami Maki, Yuko Amo, and Takeshi Usuki

Department of Material and Biological Chemistry, Faculty of Science, Yamagata University, 1-4-12 Kojirakawa-machi, Yamagata 990-8560

Received July 17, 2009; E-mail: kameda@sci.kj.yamagata-u.ac.jp

Neutron diffraction measurements were carried out on $^{14}N/^{15}N$ and H/D isotopically substituted aqueous 25 mol % urea ($x_{urea} = 0.25$) solutions in order to obtain direct experimental information on the short-range structure on the urea–urea, urea–water, and water–water interactions in highly concentrated aqueous urea solutions near saturation. Scattering cross sections observed for isotopically distinct solutions were successfully combined to derive intermolecular partial structure factors, $a_{NN}^{inter}(Q)$, $a_{NH}^{inter}(Q)$, $a_{NO(NC)}^{inter}(Q)$, $a_{HH}^{inter}(Q)$, $a_{XH}^{inter}(Q)$, and $a_{XX}^{inter}(Q)$ (X: O, N, and C), and corresponding intermolecular partial pair correlation functions. The nearest neighbor intermolecular N···O and N···H distances have been obtained as 3.14(1) and 3.42(1) Å, respectively, indicating that the amino group of the urea molecule forms hydrogen bonds with neighboring water molecules in such a highly concentrated solution. The nearest neighbor intermolecular N···N interaction was found at intermolecular distance of 4.71(5) Å with a coordination number of 3.1(5), which evidences that the hydrogen-bonded urea oligomers exist in the present solution. The nearest neighbor intermolecular O···H distance has been found to be 1.90(1) Å, which indicates that hydrogen bonds among the solvent water molecules are still preserved in the present solutions. On the other hand, corresponding O···H coordination number 0.83(1) is much smaller than that reported for room temperature liquid water. The nearest neighbor intermolecular H···H and O···O distances were determined to be 2.37(5) and 2.86(2) Å, respectively. The corresponding H···H and O···O coordination numbers were obtained as 2.0(5) and 1.4(1), respectively. These values are also much smaller than those observed for the pure water. The present results suggest that the hydrogen-bonded network among water molecules is considerably modified due to the nearest neighbor urea–water and urea–urea interactions, which can be strongly related with protein denaturation ability of the concentrated aqueous urea solutions.

Hydrogen-bonded structure in concentrated aqueous urea solution has received considerable attention because of its importance in various fields of chemical and biological sciences. Particularly, the molecular mechanism of protein denaturation by urea in concentrated aqueous solution has long been a matter of interest. Since the urea molecule has two different kinds of hydrophilic functional groups (amino- and carbonyl groups), it is important to examine the concentration dependence of the hydration structure of these functional groups. The hydration structure around the amino group has extensively been investigated by neutron diffraction with $^{14}N/^{15}N$ isotopic substitution.[1–9] The first experimental distribution function around the nitrogen atom of the urea molecule, $G_N(r)$, was obtained by Finney et al.[1–4] The number of D_2O molecules in the first hydration shell of the amino group of the urea molecule was estimated to be 7.1(5) through an integration of the observed $G_N(r)$ from $r = 2.55$ to 4.00 Å.[1–4] The $G_N(r)$ function observed for 2.0, 7.0, and 14.0 mol kg^{-1} (3.8, 12.5, and 22.2 mol %) urea solutions indicated very similar intermolecular structure around the amino group in these solutions.[5] Since the observed $G_N(r)$ is the weighted sum of N–O, N–H, N–C, and N–N partial distribution functions, deconvolution of $G_N(r)$ into contributions from these partial structure functions should be necessary to determine detailed hydration geometry of water molecules in the first hydration shell of the amino group. Moreover, observed $G_N(r)$ involves intramolecular peaks overlapping with the intermolecular distribution, which often prevent us from obtaining structural information on the urea–water interaction. In order to determine the hydration geometry of water molecules in the first hydration shell of the amino group, it is necessary to distinguish intermolecular partial distribution functions, $g_{NO}^{inter}(r)$ and $g_{NH}^{inter}(r)$, from observed $G_N(r)$ functions. A combination of the $^{14}N/^{15}N$ and H/D isotopic substitution methods is therefore indispensable. Turner et al. have reported $\Delta_N(Q)$ and corresponding $G_N(r)$ functions observed for 2.0 and 7.0 mol kg^{-1} (3.8 and 12.5 mol %) urea solutions in H_2O–D_2O mixtures.[4,5] However, definite conclusions on the nearest neighbor N–O and N–H correlations have not been drawn, probably due to relatively lower H_2O contents which would make the separation of the N–O and N–H contributions difficult. Moreover, significant overlap between the intra- and intermolecular contributions in the observed $G_N(r)$ has caused an additional difficulty in determining the hydration geometry of the water molecule around the amino group. Intermolecular N–O and N–H partial structure factors in the aqueous 15 mol % urea solution have been successfully determined by employing the null mixture of H_2O and D_2O, in which the average scattering length of

Published on the web January 29, 2010; doi:10.1246/bcsj.20090183

hydrogen atoms is set to be zero.[9] Prior to deriving the partial structure functions, the calculated intramolecular contribution within the urea molecule was subtracted from the observed total difference function, $\Delta_N(Q)$ to obtain the intermolecular difference function, $\Delta_N^{inter}(Q)$.[9] This procedure proved to be useful in reducing truncation errors associated with the Fourier transform of the $\Delta_N^{inter}(Q)$ with a rather small value of the upper Q limit ($Q_{max} = 9.6\,Å^{-1}$), because the intermolecular interference function, $\Delta_N^{inter}(Q)$, is known to be well converged at ca. $10\,Å^{-1}$ due to relatively longer intermolecular distances and larger values of the root-mean-square displacement for the intermolecular interaction between atoms. According to the analysis of intermolecular N–O and N–H partial structure factors, ca. 2 water molecules are found to form hydrogen bonds with an amino group of the urea molecule, which is consistent with the structural characteristics of the urea molecule. Interestingly, two or three more water molecules are also found to be present at just outside of the first hydration shell of the amino group. These results may explain the relatively large number of water molecules in the first hydration shell of the amino group of the urea molecule, which has been proposed by earlier neutron diffraction studies.[1–4] Recently, hydration structure around the carbonyl-carbon atom of the urea molecule has been studied by means of neutron diffraction with $^{12}C/^{13}C$ isotopically substituted aqueous 15 mol % urea solutions in D_2O.[10] On the average, 4.3(3) water molecules are hydrogen-bonded to the carbonyl-oxygen atom. This hydration number might involve water molecules binding to both the carbonyl- and the amino groups.

These results from the neutron diffraction studies for the aqueous 15 mol % urea solution indicate at least ca. 10 water molecules are present in the first hydration shell of the urea molecule. In highly concentrated aqueous urea solution, most of the water molecules should interact with the urea molecule. Since hydrogen bonds between urea and water molecules do not fit with the tetrahedral hydrogen-bonded network among water molecules because of the larger molecular size of urea and difference in the direction to form intermolecular hydrogen bonds between urea and water, the water–water structure can be significantly modified by the urea–water interaction. It is of considerable interest to investigate the intermolecular partial structure functions for more concentrated solutions. Recently, Soper et al. reported results of neutron diffraction measurements for five $^{14}N/^{15}N$ and H/D isotopically distinct 20 mol % aqueous urea solutions.[8] The empirical potential structure refinement (EPSR) analysis of observed N–X (X: O, C, N, and H), H–H, X–H, and X–X (X: O, C, and N) partial structure factors indicates that urea forms hydrogen bonds with 5.7 nearest neighbor water molecules. This implies that the number of hydrogen bonds between a urea molecule and the nearest neighbor water molecules decreases with increasing solute concentration. More recent neutron diffraction study combined with the EPSR analysis of supersaturated 30 mol % urea solutions suggested that ca. 4.1 water molecules are hydrogen-bonded to a urea molecule.[9] The EPSR analysis has an advantage of obtaining all the partial structure factors simultaneously from a limited number of observed total scattering intensities from isotopically distinct sample solutions. It is well recognized that this procedure works satisfactorily in deriving partial structure factors that occupy larger contribution in the total structure factor. However, relatively large uncertainties might be involved in the derived partial structure functions with smaller weighting factors because slight imperfection of the inelasticity correction could affect the result of the fit. On the other hand, the difference method of observed neutron scattering intensities can avoid these difficulties by taking the difference between scattering intensities of isotopically substituted sample solutions that involve identical inelasticity contribution. This may lead to more reliable determination of partial structure factor with smaller weightings in the total structure factor as discussed in the present work.

The partial distribution functions describing the water–water interaction in the highly concentrated urea solution is of particular interest relating with the protein denaturating property of the aqueous urea solution. The denaturation of a typical globular protein is considered to occur in the hydrophobic environment, which may correspond to the significant breakdown of the hydrogen-bonded interaction among water molecules. The H–H and X–H (X: O, C, and N) partial distribution functions derived from neutron diffraction measurements with H/D isotopically substituted 15.3 mol % aqueous urea solutions indicated a shift in the average hydrogen-bonded H···H distances toward the longer distance compared to that for pure water, implying that the hydrogen bonds among water molecules are partially broken in this solution.[11] On the other hand, the O_W–O_W partial distribution function, $g_{OwOw}(r)$, derived from the EPSR analysis of a supersaturated 30 mol % urea solution exhibits a very sharp first peak, which reflects hydrogen bonds among water molecules are well preserved in such a highly concentrated solution.[9] However, this could be inconsistent with the collapse of the hydrogen bonds between water molecules in highly concentrated urea solutions which has been suggested from an earlier X-ray diffraction study[12] and the hydration structure of urea in the highly concentrated solution as mentioned above. On the other hand, molecular dynamics (MD) simulations of aqueous urea solutions have shown that urea has a minor effect on bulk water structure beyond the first hydration shell of the urea molecule.[13–19] Obviously, direct experimental determination of the partial structure functions concerning the water–water interaction is therefore necessary.

The urea–urea correlation in aqueous solution has also received considerable interest in describing the structural properties of highly concentrated aqueous urea solutions. According to earlier MD simulations for 10 urea + 277 water system (3.5 mol % urea solution), oligomers of urea molecules connected with hydrogen bonds were reported.[13] However, structural properties of the urea oligomers were found to strongly depend on the initial configuration and equilibration process employed in the simulation.[13] Recent neutron diffraction with the EPSR simulation for aqueous 20 mol % urea solution proposed the formation of hydrogen-bonded chains or clusters of urea molecules was reported, which is consistent with the observed partial structure factors.[8] The intermolecular urea–urea correlation in supersaturated aqueous 30 mol % urea solutions was investigated by neutron diffraction with EPSR analysis.[9] It was found that the urea–urea interaction is characterized by a resolved first peak at 4.45 Å in the $g_{CC}(r)$

Table 1. Isotopic Composition, Average Coherent Scattering Lengths, b_N and b_H, of Nitrogen and Hydrogen Atoms, Total Cross Section, and Number Density of Samples in the Stoichiometric Unit, $[(^*N^*H_2)_2C{=}O]_{0.25}(^*H_2O)_{0.75}$, σ_t and ρ, Respectively

Sample		^{14}N /%	^{15}N /%	H /%	D /%	b_N /10^{-12} cm	b_H /10^{-12} cm	σ_t /barns	ρ /Å^{-3}
I	$[(^{14}ND_2)_2C{=}O]_{0.25}(D_2O)_{0.75}$	99.63	0.37	0.1	99.9	0.936	0.666	22.154[a)]	
II	$[(^{15}ND_2)_2C{=}O]_{0.25}(D_2O)_{0.75}$	2.0	98.0	0.1	99.9	0.650	0.666	18.920[a)]	
III	$[(^{14-15}ND_2)_2C{=}O]_{0.25}(D_2O)_{0.75}$	50.8	49.2	0.1	99.9	0.793	0.666	20.668[a)]	
IV	$[(^{14}N^0H_2)_2C{=}O]_{0.25}(^0H_2O)_{0.75}$	99.63	0.37	60.04	39.96	0.936	0.042	69.683[a)]	0.02419
V	$[(^{15}N^0H_2)_2C{=}O]_{0.25}(^0H_2O)_{0.75}$	2.0	98.0	60.04	39.96	0.650	0.042	66.040[a)]	
VI	$[(^{14}ND_2)_2C{=}O]_{0.25}(D_2O)_{0.75}$	99.63	0.37	0.1	99.9	0.936	0.666	19.288[b)]	
VII	$[(^{14}ND_2)_2C{=}O]_{0.25}(^0H_2O)_{0.75}$	99.63	0.37	64.1	35.9	0.936	0.000	68.715[b)]	
VIII	$[(^{14}ND_2)_2C{=}O]_{0.25}(^{0-2}H_2O)_{0.75}$	99.63	0.37	32.1	67.9	0.936	0.333	43.907[b)]	

a) For incident neutron wavelength of $\lambda = 1.099$ Å. b) For incident neutron wavelength of $\lambda = 1.062$ Å.

function. This suggests that urea clusters are formed in the solution,[9] however the N–N partial distribution function was not reported. Direct determination of the intermolecular N–N partial structure functions is therefore necessary to obtain further structural information on the urea clusters formed in highly concentrated aqueous solutions.

In the present paper, we describe results of neutron diffraction measurements on $^{14}N/^{15}N$ and H/D isotopically substituted 25 mol % urea solutions. Intermolecular partial structure factors, $a_{NH}^{inter}(Q)$, $a_{NO(NC)}^{inter}(Q)$, $a_{NN}^{inter}(Q)$, $a_{HH}^{inter}(Q)$, $a_{XH}^{inter}(Q)$, and $a_{XX}^{inter}(Q)$ (X: O, C, and N) and corresponding partial pair correlation functions were directly obtained from the combination of scattering cross sections observed for eight isotopically distinct sample solutions in order to obtain detailed structural information on urea–water, urea–urea, and water–water interactions in highly concentrated aqueous urea solution. Details of structural properties concerning the short-range interactions were determined through the least-squares refinement of observed intermolecular partial structure factors.

Experimental and Data Analysis

Materials. Isotopically enriched $(^{15}NH_2)_2C{=}O$ (98.0% ^{15}N, Isotech Inc.) and natural $(^{14}NH_2)_2C{=}O$ (99.6% ^{14}N, Nacalai Tesque, guaranteed grade) were deuterated by dissolving them into 10 times the molar quantity of D_2O (99.9% D, Aldrich Chemical Co., Inc.), followed by removal of water under vacuum. This procedure was repeated 4 times. The required amounts of enriched compounds were dissolved into D_2O or H_2O/D_2O mixtures to prepare eight kinds of aqueous 25 mol % urea solutions with different isotopic compositions. Each sample solution was sealed in a cylindrical fused quartz cell (12.0 mm in inner diameter and 1.1 mm in wall thickness). In order to ensure the complete subtraction of the scattering intensity from the quartz sample cell in the absorption correction, sample cells made with the same lot of fused quartz tube were employed, and carefully selected by confirming the outer diameter deviations within ±0.05 mm. Sample parameters are listed in Table 1. The coherent scattering length, scattering and absorption cross sections for nuclei, N, O, and C, were referred to those tabulated by Sears.[20] Scattering cross section for H and D nuclei calculated from observed total cross sections for liquid H_2O and D_2O,[21,22] were applied to the absorption correction of scattering intensities. A sample with the isotopic composition of the "null mixture," in which the average scattering length of hydrogen atom is zero, was prepared for the purpose of depressing enhanced uncertainties due to extremely large incoherent scattering of H.

Neutron Diffraction Measurements. Neutron diffraction measurements were carried out at 25 °C using the ISSP diffractometer 4G (GPTAS) installed at the JRR-3M reactor operated at 20 MW in the Japan Atomic Energy Agency (JAEA), Tokai, Japan. The incident neutron wavelengths, $\lambda = 1.099(4)$ and $1.062(4)$ Å, determined by Bragg reflections from the KCl powder, were employed for the diffraction measurements on sample solutions I–V and VI–VIII, respectively. Beam collimations were 40′–80′–80′ in going from the reactor to the detector. The aperture of the collimated beam was 20 mm in width and 40 mm in height. Scattered neutrons were collected over the angular range $3 \le 2\theta \le 118°$, corresponding to a scattering vector magnitude range of $0.30 \le Q \le 9.80$ and $0.31 \le Q \le 10.14$ Å^{-1} for samples I–V and VI–VIII, respectively ($Q = 4\pi \sin\theta/\lambda$). The angular step intervals were chosen to be $\Delta 2\theta = 0.5°$ in the range $3 \le 2\theta \le 40°$ and $\Delta 2\theta = 1.0°$ in the range $41 \le 2\theta \le 118°$, respectively. The preset time was 230 and 220 s for samples I–V and VI–VIII, respectively. Scattering intensities were measured for the empty cell, vanadium rod of 10 mm in diameter, and instrumental background.

Data Reduction. Observed scattering intensities from the sample solutions were corrected for instrumental background and absorption of both the sample and cell.[23] The observed count rate for the sample was converted to absolute scale by using absorption and multiple scattering corrected scattering intensities from the vanadium rod.

Absorption and multiple scattering corrections for samples containing large amounts of hydrogen (and also deuterium) atom have often been a subject of discussion. The total cross section of liquid H_2O for incident neutron wavelength of $\lambda = 1.1$ Å is calculated to be 169 barn by employing bound cross sections for H and O atoms from literature values,[20] while the corresponding experimental value is only 70 barn[22] due to substantial inelasticity effect mainly caused by the hydrogen atoms. Similarly, the observed total cross section of liquid D_2O is reported to be 13 barn,[22] which is also much smaller than the calculated value, 20 barn.[20] In correction procedures for absorption and multiple scattering, it is necessary to employ the realistic value for the total cross section of the sample. In fact, it has been indicated that the use of bound cross sections for H and D atoms for the absorption correction causes an overestimation of the amplitude in the intramolecular interference term while a good agreement is obtained between the theoretical intramolecular interference amplitude and the observed value corrected by the use of experimental total cross sections for H and D atoms.[24–28] Since the magnitude of multiple scattering from a sample is known to become much larger for a hydrogeneous sample contained in a

cylindrical sample cell with large diameter due to the extremely large scattering cross section of the H atom, a very thin slab cell[29] and a cylindrical cell with a smaller diameter[30] have been employed to reduce the multiple scattering contribution. We tentatively estimated the multiple scattering contribution from a ^{14}N–^{0}H solution (sample IV) contained in a cylindrical cell with a diameter of 12 mm, which is much larger than that employed in the previous studies. The multiple scattering contribution for the present sample solution is estimated to be 52% of the observed scattering intensity by using a simple isotropic approximation[31] with the experimental values of the cross sections of H and D.[22] Although this estimation could be rather approximated, it may imply that multiple scattering contribution is at most ca. 1/2 of observed scattering intensity under the present experimental conditions and we are able to extract the interference term from observed scattering data in sufficient accuracy even if we employed relatively large diameter for the sample cell. In the case of applying observed cross sections for H and D to the absorption correction, we should pay attention to the fact that there might be differences in the effective cross section of the hydrogen atom within the water molecule and that within the urea molecule. In order to check the overall normalization of the observed scattering cross section for the sample solution, least-squares fitting was performed for the observed intramolecular interference term, which will be discussed in a later section.

Although several theoretical approaches have been proposed in the literature,[31–37] no generalized procedure seems to be established for multiple and inelasticity corrections in aqueous solutions involving $^{*}H_2O$ and $(N^{*}H_2)_2C{=}O$, such as the present sample. Previous Monte Carlo calculations have indicated that observed scattering intensities in liquid formic acid containing a considerable amount of H depend markedly on Q, reflecting the strong Q-dependence of multiple scattering terms.[32] Present samples exhibit also strong Q-dependent scattering intensities due to the inelasticity effect of H. Since it is difficult to evaluate the multiple scattering contribution for the present sample adequately by a simple isotropic approximation of Blech and Averbach,[31] we employ in the present analysis an empirical method of a polynomial expansion which has been frequently applied for data correction for samples containing complex molecules, such as liquid methanol,[38,39] ethanol,[40] and D-glycerol.[41] More recently, Bellissent-Funel et al. have indicated that the polynomial expansion method supplies reliable inelasticity corrections for liquid D_2O and H_2O/D_2O mixtures.[42] Consequently, in the present analysis, the sum of observed intensities of coherent (except for the interference term), incoherent and multiple scattering contributions was treated as the self-scattering term which can be well approximated by the polynomial expansion into even-order powers of Q. After preliminary analyses, it was revealed that the maximum order of the eighth power was adequate to approximate the self scattering term observed for samples involving large amount of ^{0}H. The calculated self term was a smoothly and monotonically varying function and did not exhibit sudden variation with Q.

In the present analysis, intermolecular partial structure factors are derived from the difference function between scattering cross sections observed for isotopically distinct sample solutions, which requires high accuracy of the absolute intensity for observed interference amplitudes as well as good counting statistics of the scattering data. Therefore, we have to check the absolute amplitude of interference term by using oscillational amplitude of the intramolecular interference term, which can readily be calculated from known molecular geometries and composition of sample solutions. Since it is well established that the amplitude of the intermolecular interference term decreases much faster than that of intramolecular one with increasing Q-value, interference features appearing at higher-Q regions of the observed scattering cross section can be regarded as the contribution from intramolecular interference term. Then, we introduce renormalization factor, α, in order to confirm absolute amplitude of the observed interference term and also to verify validity of absorption correction procedure employed in the present analysis. The renormalization factor was determined by procedures described below.

The observed total scattering cross section, $(d\sigma/d\Omega)_0^{obs}$, involving intra- and intermolecular interference term, and the self term can be written as the following equation:

$$(d\sigma/d\Omega)_0^{obs} = \alpha[(d\sigma/d\Omega)_{int}^{intra} + (d\sigma/d\Omega)_{int}^{inter} + (d\sigma/d\Omega)^{self}] \quad (1)$$

$(d\sigma/d\Omega)_{int}^{intra}$ and $(d\sigma/d\Omega)_{int}^{inter}$ stand for intra- and intermolecular interference terms, respectively. $(d\sigma/d\Omega)_{int}^{intra}$ scaled in the stoichiometric unit, $[(^{*}N^{*}H_2)_2C{=}O]_x(^{*}H_2O)_{1-x}$, is represented by the sum of contributions from urea and water molecules, i.e.,

$$(d\sigma/d\Omega)_{int}^{intra} = x(d\sigma/d\Omega)_{int}^{intra}(\text{for urea}) + (1-x)(d\sigma/d\Omega)_{int}^{intra}(\text{for water}) \quad (2)$$

where

$$(d\sigma/d\Omega)_{int}^{intra}(\text{for urea}) = \sum\sum_{i\neq j} b_i b_j \exp(-l_{ij}^2 Q^2/2)\sin(Qr_{ij})/(Qr_{ij}) \quad (3)$$

and

$$(d\sigma/d\Omega)_{int}^{intra}(\text{for water}) = 4b_O b_H \exp(-l_{OH}^2 Q^2/2)\sin(Qr_{OH})/(Qr_{OH}) + 2b_H^2 \exp(-l_{HH}^2 Q^2/2)\sin(Qr_{HH})/(Qr_{HH}) \quad (4)$$

Parameters, l_{ij} and r_{ij} denote the root-mean-square displacement and internuclear distance for the i–j pair, respectively. Values of r_{ij} and l_{ij} for the urea molecule were taken from the literature determined from single crystal neutron diffraction[43] and from values calculated for related molecules,[44,45] respectively. Intramolecular parameters for the water molecule, r_{OH}, r_{HH}, l_{OH}, and l_{HH}, were those determined from neutron diffraction studies for liquid heavy water.[36,46,47] The Q-dependence of the self term in eq 1 was approximated by the polynomial expansion of Q as mentioned above:

$$(d\sigma/d\Omega)^{self} = a_1 + a_2 Q^2 + a_3 Q^4 + a_4 Q^6 + a_5 Q^8 \quad (5)$$

Coefficients a_1–a_5 in eq 5 and the normalization factor α in eq 1 were simultaneously determined by a least-squares fit to the observed total scattering cross section in the range of $3.0 \leq Q \leq 9.8\ \text{Å}^{-1}$. The fitting procedure was performed by the SALS program.[48] Values of α for D_2O solutions, I, II, III, and VI, were determined to be 0.98(1), 1.09(8), 1.06(1), and 0.99(1), respectively. These values are close to unity, which indicates the present absorption correction was adequately carried out. For $^{0}H_2O$ and $^{0\text{–}2}H_2O$ solutions, the renormalization factor was found to be 0.81(1), 0.91(1), 0.80(1), and 0.86(1) for sample solutions IV, V, VII, and VIII, respectively. These results indicate that normalization errors associated with the absorption correction are roughly estimated to 10–20% for samples containing large amount of H. Renormalized scattering cross section, $(d\sigma/d\Omega)^{obs}$, was evaluated by the following equation:

$$(d\sigma/d\Omega)^{obs} = (d\sigma/d\Omega)_0^{obs}/\alpha \quad (6)$$

Table 2. Weighting Factors for Partial Structure Factors in the First- and Second-Order Difference Functions

Difference function	A/barns	B/barns	C/barns	D/barns
${}^{D}\Delta_N(Q)$ (I − II)	0.1660	0.4763	0.0475	0.1134
${}^{0H}\Delta_N(Q)$ (IV − V)	0.1660	0.0300	0.0475	0.1134
${}^{D}\Delta'_N(Q)$ (I − III)	0.0830	0.2383	0.0238	0.0618
${}^{D}\Delta''_N(Q)$ (III − II)	0.0830	0.2383	0.0238	0.0516
${}^{D}\Delta_N(Q) - {}^{0H}\Delta_N(Q)$	0	0.4463	0	0
${}^{D}\Delta'_N(Q) - {}^{D}\Delta''_N(Q)$	0	0	0	0.0102

The first-order difference functions,[49–52] $\Delta_N(Q)$, is defined as the numerical difference of renormalized observed scattering cross sections from sample solutions, that are identical in isotopic composition of hydrogen atoms and different in isotopic composition of amino-nitrogen atoms within the urea molecule:

$$ {}^{D}\Delta_N(Q) = (d\sigma/d\Omega)^{obs}(\text{for sample I}) - (d\sigma/d\Omega)^{obs}(\text{for sample II}) \quad (7) $$

$$ {}^{0H}\Delta_N(Q) = (d\sigma/d\Omega)^{obs}(\text{for sample IV}) - (d\sigma/d\Omega)^{obs}(\text{for sample V}) \quad (8) $$

Similarly, difference functions, ${}^{D}\Delta'_N(Q)$ and ${}^{D}\Delta''_N(Q)$, were obtained from the difference in scattering cross sections observed for samples I − III, and III − II, respectively. They were used in deriving the N–N partial structure factor:

$$ {}^{D}\Delta'_N(Q) = (d\sigma/d\Omega)^{obs}(\text{for sample I}) - (d\sigma/d\Omega)^{obs}(\text{for sample III}) \quad (9) $$

$$ {}^{D}\Delta''_N(Q) = (d\sigma/d\Omega)^{obs}(\text{for sample III}) - (d\sigma/d\Omega)^{obs}(\text{for sample II}) \quad (10) $$

$\Delta_N(Q)$, scaled at the stoichiometric unit, $[(*N*H_2)_2C{=}O]_x$-$(*H_2O)_{1-x}$, can be expressed as the weighted sum of four partial structure factors:

$$ \Delta_N(Q) = A[a_{NO}(Q) - 1] + B[a_{NH}(Q) - 1] + C[a_{NC}(Q) - 1] + D[a_{NN}(Q) - 1] \quad (11) $$

where, $A = 4x(b_N - b'_N)b_O$, $B = 8x(1+x)(b_N - b'_N)b_H$, $C = 4x^2(b_N - b'_N)b_C$, and $D = 4x^2(b_N^2 - b'^2_N)$, respectively. Weighting factors *A–D* in eq 11 are numerically listed in Table 2. The intramolecular interference contribution, ${I_N}^{intra}(Q)$, arising from the N···α pair within the urea molecule is calculated by

$$ {I_N}^{intra}(Q) = \sum 2c_N b_\alpha (b_N - b'_N) \times \exp(-{l_{N\alpha}}^2 Q^2/2)\sin(Qr_{N\alpha})/(Qr_{N\alpha}) \quad (12) $$

where, c_N denotes the number of N atoms in the stoichiometric unit. The calculated ${I_N}^{intra}(Q)$ was then subtracted from observed $\Delta_N(Q)$ to obtain the intermolecular difference function, ${\Delta_N}^{inter}(Q)$,

$$ {\Delta_N}^{inter}(Q) = \Delta_N(Q) - {I_N}^{intra}(Q) \quad (13) $$

Distribution function, $G_N(r)$, around the nitrogen atom is obtained by the Fourier transform of observed $\Delta_N(Q)$,

$$ G_N(r) = 1 + (A+B+C+D)^{-1}(2\pi^2\rho r)^{-1} \times \int_0^{Q_{max}} Q\Delta_N(Q)\sin(Qr)dQ = [Ag_{NO}(r) + Bg_{NH}(r) + Cg_{NC}(r) + Dg_{NN}(r)] \times (A+B+C+D)^{-1} \quad (14) $$

The upper limit of integral, Q_{max}, was set to 9.80 Å^{-1}. The intermolecular distribution function, ${G_N}^{inter}(r)$, was evaluated by the Fourier transform of ${\Delta_N}^{inter}(Q)$.

In the preliminary analysis, it was found that unphysical ripples appearing in the $G_N(r)$ were much reduced by applying a moving average procedure to the observed $\Delta_N(Q)$. The number of the data points adopted in the data-averaging procedure was decided carefully considering the following criteria. (a) Oscillatory features involved in the observed $\Delta_N(Q)$ should not be smeared. This was confirmed by the sharpness of the intramolecular peaks appearing in the transformed $G_N(r)$. (b) Unphysical ripples in $G_N(r)$ are sufficiently suppressed. In the present analysis, a three-point moving average was adopted for the observed $\Delta_N(Q)$ and used for subsequent analysis.

The second-order difference[50,52] between ${}^{D}{\Delta_N}^{inter}(Q)$ and ${}^{0H}{\Delta_N}^{inter}(Q)$ gives the intermolecular N–H partial structure factor, ${a_{NH}}^{inter}(Q)$:

$$ {}^{D}{\Delta_N}^{inter}(Q) - {}^{0H}{\Delta_N}^{inter}(Q) = 8x(1+x)(b_N - b'_N)(b_D - b_{0H})[{a_{NH}}^{inter}(Q) - 1] \quad (15) $$

The intermolecular N–N partial structure factor, ${a_{NN}}^{inter}(Q)$, was derived from the second-order difference between ${}^{D}{\Delta'_N}^{inter}(Q)$(I − III) and ${}^{D}{\Delta''_N}^{inter}(Q)$(III − II). In the present study, the coherent scattering length of the sample III, b''_N, was set to be the mean value of those for sample I and II, i.e., $(b_N + b'_N)/2$.

$$ {}^{D}{\Delta'_N}^{inter}(Q)(\text{I} - \text{III}) - {}^{D}{\Delta''_N}^{inter}(Q)(\text{III} - \text{II}) = 2x^2(b_N - b'_N)^2[{a_{NN}}^{inter}(Q) - 1] \quad (16) $$

The weighted sum of intermolecular N–O and N–C partial structure factors was given by subtracting contributions from intermolecular N–N and N–H partial structure factors from the observed ${}^{0H}{\Delta_N}^{inter}(Q)$.

$$ {}^{0H}{\Delta_N}^{inter}(Q) - 0.1134[{a_{NN}}^{inter}(Q) - 1] - 0.0300[{a_{NH}}^{inter}(Q) - 1] = 0.1660[{a_{NO}}^{inter}(Q) - 1] + 0.0475[{a_{NC}}^{inter}(Q) - 1] \quad (17) $$

In the present experimental condition, the N–O contribution is dominated in the resulting partial structure function.

Intermolecular H–H, X–H, and X–X (X: O, C, and N) partial structure factors were obtained from the combination of intermolecular interference terms observed for samples VI, VII, and VIII:

$$ (d\sigma/d\Omega)_{int}{}^{inter}(\text{for VI}) + (d\sigma/d\Omega)_{int}{}^{inter}(\text{for VII}) - 2(d\sigma/d\Omega)_{int}{}^{inter}(\text{for VIII}) = 2(1+x)^2 {b_D}^2[{a_{HH}}^{inter}(Q) - 1] \quad (18) $$

$$ 4(d\sigma/d\Omega)_{int}{}^{inter}(\text{for VIII}) - (d\sigma/d\Omega)_{int}{}^{inter}(\text{for VI}) - 3(d\sigma/d\Omega)_{int}{}^{inter}(\text{for VII}) = 4(1+x)(2xb_N + xb_C + b_O)b_D[{a_{XH}}^{inter}(Q) - 1] \quad (19) $$

and

$$ (d\sigma/d\Omega)_{int}{}^{inter}(\text{for VII}) = (2xb_N + xb_C + b_O)^2[{a_{XX}}^{inter}(Q) - 1] \quad (20) $$

The intermolecular partial pair correlation function, ${g_{ij}}^{inter}(r)$, was evaluated by the Fourier transform of observed ${a_{ij}}^{inter}(Q)$:

$$ {g_{ij}}^{inter}(r) = 1 + (2\pi^2\rho r)^{-1}\int_0^{Q_{max}} Q[{a_{ij}}^{inter}(Q) - 1]\sin(Qr)dQ \quad (21) $$

The upper limit of the integral, Q_{max}, was taken to be 9.80 Å^{-1} for ${g_{NN}}^{inter}(r)$, ${g_{NH}}^{inter}(r)$, and ${g_{NO(NC)}}^{inter}(r)$ $(=0.78{g_{NO}}^{inter}(r) + 0.22{g_{NC}}^{inter}(r))$ functions. The value of $Q_{max} = 10.14$ Å^{-1}, was employed in evaluation of ${g_{HH}}^{inter}(r)$, ${g_{XH}}^{inter}(r)$, and ${g_{XX}}^{inter}(r)$.

The intermolecular distance, root-mean-square displacement, and coordination number, r_{ij}, l_{ij}, and n_{ij}, for the i–j atom pair, were

determined by the least-squares fit of the observed $a_{ij}^{inter}(Q)$ to the corresponding calculated values, $a_{ij}^{calc}(Q)$, involving the contribution from short- and long-range interactions:[53–55]

$$a_{ij}^{calc}(Q) - 1 = \sum \beta_{ij} n_{ij} \exp(-l_{ij}^2 Q^2/2) \sin(Qr_{ij})/(Qr_{ij}) + 4\pi\rho \exp(-l_0^2 Q^2/2)[Qr_0 \cos(Qr_0) - \sin(Qr_0)]Q^{-3} \quad (22)$$

The long-range parameter, r_0, denotes the distance beyond which uniform distribution of atoms is assumed. The parameter, l_0, describes sharpness of the boundary at r_0. The coefficient, β_{ij}, for the N–N, N–H, and H–H partial structure factors is given by $\beta_{ij} = c_j^{-1}$, where c_j denotes the number of atom j in the stoichiometric unit, $[(NH_2)_2C{=}O]_x(H_2O)_{1-x}$. For the N–O (N–C) partial structure, the following value is employed.

$$\beta_{Nj} = c_j b_j (x b_C + b_O)^{-1} \quad (23)$$

For the X–H partial structure factor, the coefficient β_{iH} is written as

$$\beta_{iH} = 2c_i b_i (1 + x)(2x b_N + x b_C + b_O)^{-1} \quad (24)$$

The coefficient, β_{ij}, for the X–X partial structure factor is evaluated by

$$\beta_{ij} = (2 - \delta_{ij}) c_i b_i b_j (2x b_N + x b_C + b_O)^2 \quad (25)$$

The fitting procedure was made using the SALS program[48] in the range of $0.30 \le Q \le 9.80\,\text{Å}^{-1}$ for $a_{NN}^{inter}(Q)$, $a_{NH}^{inter}(Q)$, and $a_{NO(NC)}^{inter}(Q)$ functions. For $a_{HH}^{inter}(Q)$, $a_{XH}^{inter}(Q)$, and $a_{XX}^{inter}(Q)$ functions, fitting range of $0.31 \le Q \le 10.14\,\text{Å}^{-1}$ was employed.

Results and Discussion

The First-Order Difference Function. Scattering cross sections observed for sample solutions I to V are shown in Figure 1. The overall features of $(d\sigma/d\Omega)^{obs}$ with different $^{14}N/^{15}N$ ratio look very similar, however, a systematic difference in the intensity can be observed around the first diffraction peak at around $Q = 2\,\text{Å}^{-1}$, which corresponds to the difference in scattering length of the amino-nitrogen atom in sample solutions. Decrease in the intensity of $(d\sigma/d\Omega)^{obs}$ at a higher-Q region is attributable to the inelasticity effect, which is more pronounced for ^0H_2O solutions involving large amount of H. Observed difference functions, $^D\Delta_N(Q)$ (sample I − sample II) and $^{0H}\Delta_N(Q)$ (sample IV − sample V), and corresponding distribution function around the amino-nitrogen atom within urea molecule, $^DG_N(r)$ and $^{0H}G_N(r)$, are shown in Figures 2 and 3, respectively. Interference features appearing in the total difference function, $^D\Delta_N(Q)$ (Figure 2a), for D_2O solutions are in good agreement with those reported for 15 mol % urea–D_2O solutions observed by the same diffractometer as that employed in the present study.[7] The present $^D\Delta_N(Q)$ is also very similar to that observed for 12.5 and 22.2 mol % urea–D_2O solutions observed using different neutron spectrometers.[5] These observation may indicate that the hydration structure around the amino group in the present highly concentrated solution has a similarity with those observed for more dilute solutions. Interference amplitude in the present $^{0H}\Delta_N(Q)$ (Figure 2d) is relatively small reflecting the smaller average coherent scattering length of the hydrogen atom. Although the data points in observed $^{0H}\Delta_N(Q)$ are somewhat scattered due to large incoherent scattering contribution from H atom in the observed scattering cross section, the first peak at $Q \approx 2\,\text{Å}^{-1}$ and

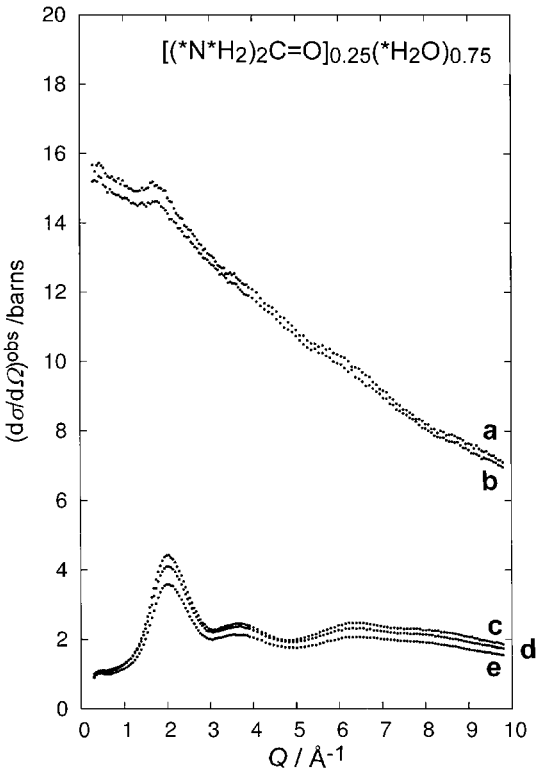

Figure 1. Scattering cross section, $(d\sigma/d\Omega)^{obs}$, observed for aqueous 25 mol % urea solutions with different isotopic ratios of $^{14}N/^{15}N$ and H/D. (a) ^{14}N–^0H, (b) ^{15}N–^0H, (c) ^{14}N–D, (d) $^{14-15}N$–D, and (e) ^{15}N–D.

oscillation extending to the larger-Q region are obviously identified. In the next step of analysis, calculated intramolecular interference term, $I_N^{intra}(Q)$ (Figures 2b and 2e), was subtracted from the observed $^D\Delta_N(Q)$ and $^{0H}\Delta_N(Q)$. The normalization factor for the observed $\Delta_N(Q)$, γ, defined by $\Delta_N(Q) = \gamma \times I_N^{intra}(Q)$ (in the sufficiently high-Q region) was estimated to be $\gamma = 1.1 \pm 0.1$ and 1.0 ± 0.1 for $^D\Delta_N(Q)$ and $^{0H}\Delta_N(Q)$, respectively, through the least-squares fit in the range of $5.0 \le Q \le 9.8\,\text{Å}^{-1}$, where contribution from the intramolecular interference term is dominant. The results indicate that present data correction and normalization procedures were adequately carried out, overall normalization error in the present $\Delta_N(Q)$ is roughly estimated to be within 10%. Intermolecular difference functions, $^D\Delta_N^{inter}(Q)$ (Figure 2c) and $^{0H}\Delta_N^{inter}(Q)$ (Figure 2f) are both characterized by well-defined first diffraction peak at $Q \approx 2\,\text{Å}^{-1}$ and the second peak located at $Q \approx 4\,\text{Å}^{-1}$.

Total and intermolecular distribution functions for D_2O solutions, $^DG_N(r)$ and $^DG_N^{inter}(r)$, are shown in Figures 3a and 3b, respectively. The first peak at $r \approx 1$ Å in the present $^DG_N(r)$ is mainly attributable to the intramolecular N–D interaction within urea. Contribution from the intramolecular N–C interaction may be included in the higher-r side shoulder of this first peak. The second peak at $r \approx 2.3$ Å can be ascribed to the sum of contributions from intramolecular non-bonding N···O, N···D, and N···N interactions. The first peak at $r \approx 1.2$ Å in the present $^{0H}G_N(r)$ is assigned mainly to the intramolecular N–C contribution. This peak should also involve small contribution from the intramolecular N–D contribution corre-

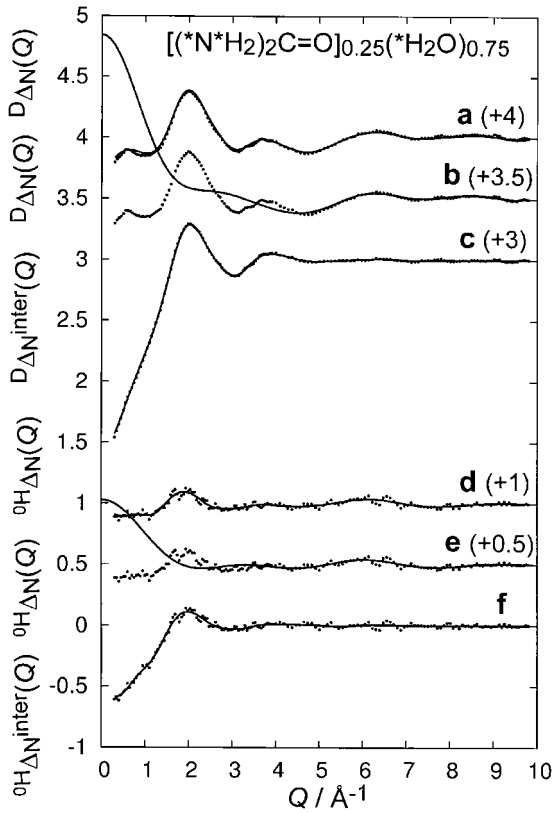

Figure 2. (a) Difference function, ${}^{D}\Delta_{N}(Q)$, observed for aqueous 25 mol % urea solutions in D_2O (dots). The back Fourier transform of ${}^{D}G_{N}(r)$ shown by the solid line in Figure 3a (solid line). (b) The observed ${}^{D}\Delta_{N}(Q)$ (dots). The intramolecular contribution within the urea molecule, $I_{N}^{intra}(Q)$ (solid line). (c) The intermolecular difference function, ${}^{D}\Delta_{N}^{inter}(Q)$ (dots). The back Fourier transform of ${}^{D}G_{N}^{inter}(r)$ shown by the solid line in Figure 3b (solid line). (d)–(f) The same notations as in (a)–(c) except for aqueous 25 mol % urea solutions in ${}^{0}H_2O$.

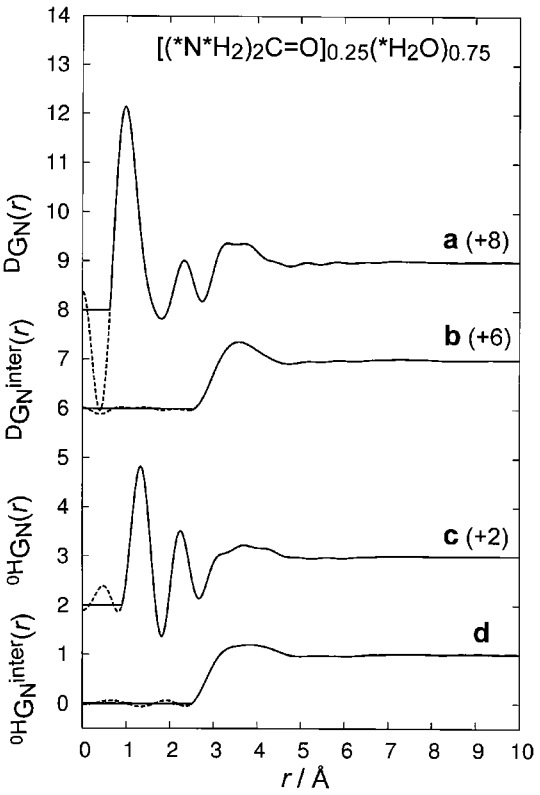

Figure 3. (a) The total and (b) intermolecular distribution functions around the amino-nitrogen atom of the urea molecule, ${}^{D}G_{N}(r)$ and ${}^{D}G_{N}^{inter}(r)$, respectively, observed for 25 mol % urea solutions in D_2O. (c) and (d) The same notations as in (a) and (b), respectively, except for ${}^{0}H_2O$ solutions.

sponding to the small value of the b_H for samples IV and V (Table 1). The second peak in the present ${}^{0H}G_{N}(r)$ seems relatively larger than that appearing in the ${}^{D}G_{N}(r)$ due to the smaller value of $A + B + C + D$ used in evaluating the ${}^{0H}G_{N}(r)$ (Table 2 and eq 14). The intermolecular distribution function, ${}^{D}G_{N}^{inter}(r)$ (Figure 3b), is characterized by a broad first peak located at $r \approx 3.6$ Å. On the other hand, the first peak in the ${}^{0H}G_{N}^{inter}(r)$ (Figure 3d) looks more smeared, reflecting the difference in the N–H contribution involved in these distribution functions. The second-order difference function, ${}^{D}\Delta_{N}^{inter}(Q) - {}^{0H}\Delta_{N}^{inter}(Q)$, can be directly connected with the intermolecular N–H partial structure factor, $a_{NH}^{inter}(Q)$.

Intermolecular N–N Partial Structure Functions. Intermolecular difference functions evaluated from differences in scattering cross sections between samples I − III (${}^{D}\Delta'_{N}{}^{inter}(Q)$) and III − II (${}^{D}\Delta''_{N}{}^{inter}(Q)$), are shown in Figures 4a and 4b, respectively. The intermolecular N–N partial structure factor, $a_{NN}^{inter}(Q)$, was derived by the second-order difference between observed ${}^{D}\Delta'_{N}{}^{inter}(Q)$ and ${}^{D}\Delta''_{N}{}^{inter}(Q)$ (Table 2). The data points of observed $a_{NN}^{inter}(Q)$ (Figure 4c) are rather scattered due to statistical uncertainties, however the first diffraction peak at $Q \approx 1.5$ Å^{-1} and oscillational features extending to higher-Q region can be identified. Figures 5a and 5b show intermolecular distribution functions, $G'_{N}{}^{inter}(r)$ and $G''_{N}{}^{inter}(r)$, respectively. Structural features in these distribution functions look very similar however a small difference can be pointed out in the intensity of observed $G_{N}^{inter}(r)$ in the shallow local minimum at $r \approx 5$ Å, which corresponds to the first peak in observed intermolecular N–N partial pair correlation function, $g_{NN}^{inter}(r)$, which is represented in Figure 5c. Slightly asymmetric shape of the first N···N peak indicates that this peak cannot be reproduced by a single intermolecular interaction. Beyond this first peak, distribution of N atoms around an N atom seems to approach random. Intermolecular structural parameters have been determined from the least-squares fitting analysis of observed intermolecular N–N partial structure factor, which is shown in Figure 6a. The fitting procedure was performed in the range of $0.3 \leq Q \leq 9.8$ Å^{-1} with the SALS program[48] under an assumption that the statistical uncertainties distribute uniformly.

Final values of all independent parameters are summarized in Table 3. The present value of the nearest neighbor N···N distance, $r_{NN} = 4.71(5)$ Å, is in good agreement with that reported in the crystalline state ($r_{NN} = 4.7$ Å),[43] in which urea molecules are packed in head to tail or linear configuration. The second nearest neighbor N···N distance, $r_{NN} = 5.22(9)$ Å, is also consistent with the second nearest neighbor N···N distance

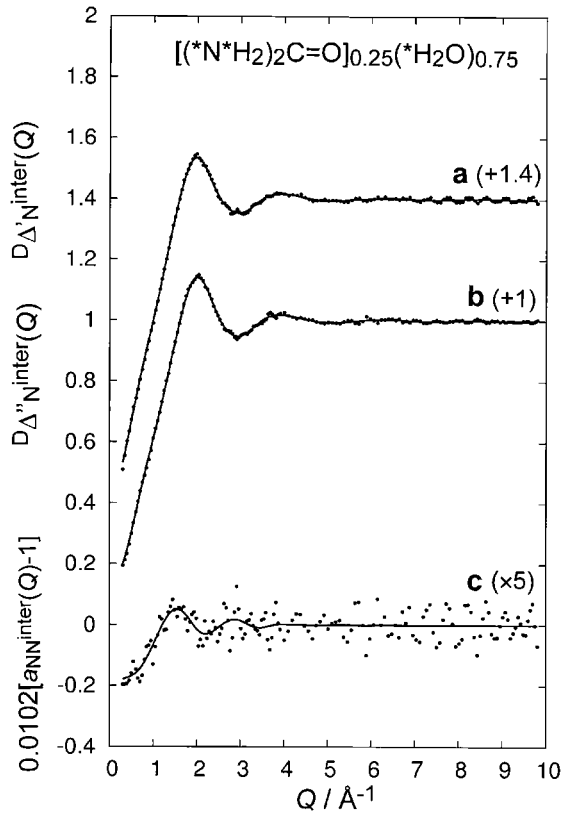

Figure 4. The intermolecular difference function derived from samples (a) I − III and (b) III − II, ${}^{D}\Delta'_{N}{}^{inter}(Q)$ and ${}^{D}\Delta''_{N}{}^{inter}(Q)$, respectively. The back Fourier transform of ${}^{D}G'_{N}{}^{inter}(r)$ and ${}^{D}G''_{N}{}^{inter}(r)$ shown by the solid line in Figures 5a and 5b, respectively. (c) Intermolecular N–N partial structure factor, $a_{NN}{}^{inter}(Q)$ (dots). The back Fourier transform of $g_{NN}{}^{inter}(r)$ shown by the solid line in Figure 5c (solid line).

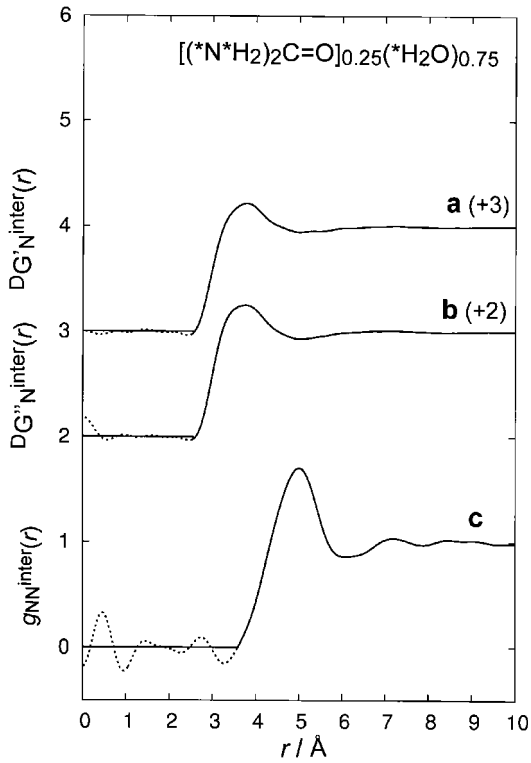

Figure 5. The intermolecular distribution function around the amino-nitrogen atom (a) ${}^{D}G'_{N}{}^{inter}(r)$ and (b) ${}^{D}G''_{N}{}^{inter}(r)$. (c) Intermolecular N–N partial pair correlation function, $g_{NN}{}^{inter}(r)$.

in urea dimer of the linear configuration. On the other hand, the present intermolecular nearest neighbor N···N distance is also close to the second nearest neighbor N···N distance in the cyclic dimer ($r_{NN} = 3.4$, 4.8×2, and 6.9 Å) which has been predicted by MD simulation studies for more dilute aqueous urea solutions.[13,19,56] According to the MD results, formation of urea cyclic dimer has been evidenced by an obvious first peak appearing at $r = 3.4$–3.6 Å in the intermolecular N–N partial pair correlation function.[13,19] No indication of the N···N peak at $r = 3.4$–3.6 Å can be found in the present experimental $g_{NN}{}^{inter}(r)$. The relatively large value of the present rms displacement for the intermolecular nearest neighbor N···N interaction ($l_{NN} = 0.35(2)$ Å) may imply that a variety of the urea–urea configurations are present in the concentrated aqueous urea solution. These results suggest that the urea–urea contact extensively occurs in the aqueous 25 mol % urea solution. Since the molecular faces of the urea molecule (conjugated π electrons) have hydrophobic property, the formation of hydrogen-bonded urea oligomers is likely to make the interaction between urea molecule and hydrophobic side chains of peptide more favorable. This suggests that the denatured protein can be stabilized by the presence of the urea oligomers.

Table 3. Results of the Least-Squares Refinement for Intermolecular Partial Structure Factors, $a_{NN}{}^{inter}(Q)$, $a_{NH}{}^{inter}(Q)$, and $a_{NO(NC)}{}^{inter}(Q)$, Observed for Aqueous 25 mol % Urea Solutions[a)]

		$a_{NN}{}^{inter}(Q) - 1$	$a_{NH}{}^{inter}(Q) - 1$	$a_{NO(NC)}{}^{inter}(Q) - 1$
Short-range	i–j	N–N	N–H	N–O
	r_{ij}/Å	4.71(5)	3.42(1)	3.14(1)
	l_{ij}/Å	0.35(2)	0.305(3)	0.28(1)
	n_{ij}	3.1(5)	8.3(4)	2.2(1)
	i–j	N–N	N–H	N–C
	r_{ij}/Å	5.22(9)	4.01(3)	4.09(3)
	l_{ij}/Å	0.54(7)	0.31(2)	0.26(1)
	n_{ij}	5(1)	5.2(3)	1.1(1)
	i–j	—	—	N–O
	r_{ij}/Å	—	—	3.77(1)
	l_{ij}/Å	—	—	0.45(1)
	n_{ij}	—	—	9.3(2)
Long-range	r_0/Å	5.8(3)	4.18(2)	4.74(2)
	l_0/Å	0.7(2)	0.67(2)	0.58(2)

a) Estimated errors are given in parentheses.

Intermolecular N–H and N–O (N–C) Partial Structure Functions. The intermolecular N–H partial structure factor, $a_{NH}{}^{inter}(Q)$, was obtained by taking the second-order difference between observed ${}^{D}\Delta_{N}{}^{inter}(Q)$ (sample I − sample II) and ${}^{0H}\Delta_{N}{}^{inter}(Q)$ (sample IV − sample V), which is shown in Figure 6b. The intermolecular N–H partial pair correlation

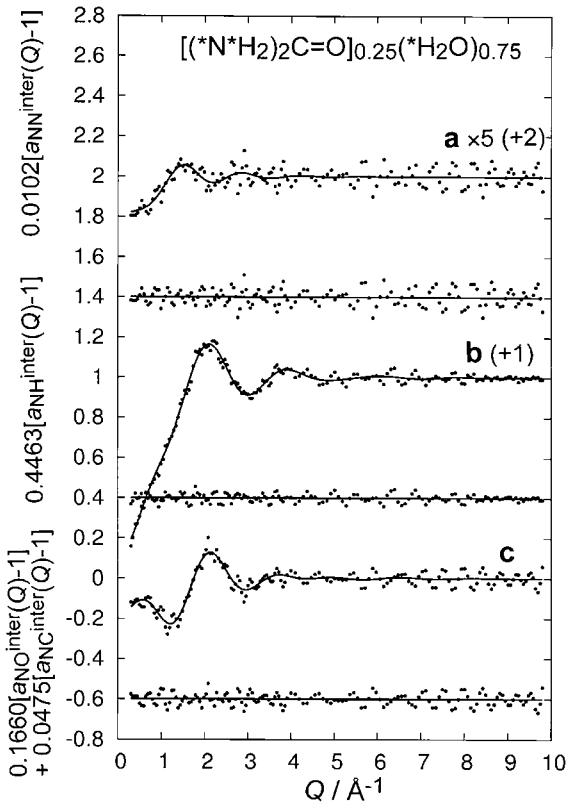

Figure 6. Intermolecular (a) N–N, (b) N–H, and (c) N–O (N–C) partial structure factors observed for aqueous 25 mol % urea solutions (dots). The best-fit of calculated interference terms in eq 22 (solid line). The difference between observed and calculated interference functions is given below.

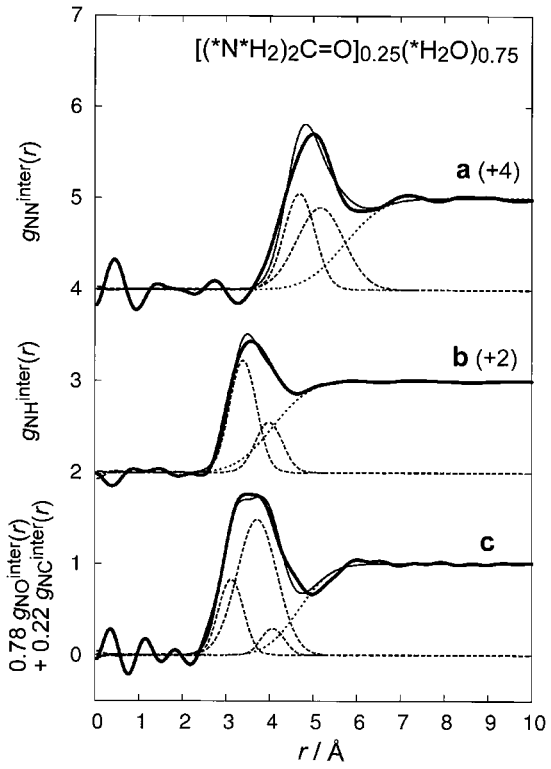

Figure 7. Intermolecular (a) N–N, (b) N–H, and (c) N–O (N–C) partial pair correlation functions observed for aqueous 25 mol % urea solutions (thick solid line). Fourier transform of the best-fit of calculated interference terms shown in Figure 6 (thin solid line). Short- and long-range components are shown by broken and dotted lines, respectively.

function, $g_{NH}^{inter}(r)$, is represented in Figure 7b. The present $g_{NH}^{inter}(r)$, is characterized by a rather broadened first peak at $r = 3.5$ Å. Beyond this first peak, the distribution of atoms approaches to random. The overall shape of the present $g_{NH}^{inter}(r)$ looks very similar to that observed for the aqueous 15 mol % urea solution.[7] In the preliminary analysis, it was found that at least two short-range interactions were needed to reproduce the present $a_{NH}^{inter}(Q)$ and corresponding $g_{NH}^{inter}(r)$ functions. It should be noted that the present $a_{NH}^{inter}(Q)$ and $g_{NH}^{inter}(r)$ functions involve contributions from both N–H(water) and N–H(urea) pairs. In order to obtain quantitative information on the short-range structure of intermolecular N···H interaction, the least-squares fitting analysis was adopted for the observed $a_{NH}^{inter}(Q)$. Two short-range interactions and a long-range interaction were taken into account in the model function employed in the fitting procedure. Final values of all independent parameters are summarized in Table 3. The present value of the nearest neighbor intermolecular N···H distance, $r_{NH} = 3.42(1)$ Å, is in excellent agreement with that observed in aqueous 15 mol % urea solution,[7] suggesting that the first hydration shell of the amino group of urea molecule is maintained in such a highly concentrated solution.

The weighted sum of intermolecular N–O and N–C partial structure factors, $a_{NO(NC)}^{inter}(Q)$, was derived by subtracting $a_{NN}^{inter}(Q)$ and $a_{NH}^{inter}(Q)$ contributions from observed ${}^{0H}\Delta_N^{inter}(Q)$, which is shown in Figure 6c. Under the present experimental conditions, contribution from the N–O partial structure factor occupies ca. 78% of the derived partial structure factor, the obtained partial pair correlation function can be approximated as the N–O partial pair correlation function. The observed intermolecular partial pair correlation function, $0.78g_{NO}^{inter}(r) + 0.22g_{NC}^{inter}(r)$, is shown in Figure 7c. The present distribution function is characterized by a well-defined first peak at around $r = 3.5$ Å. The long-range region of the distribution function beyond $r > 6$ Å is well approximated as the random distribution. The position of the first peak is significantly longer than typical hydrogen-bonded N–H···O distance, $r_{N-H\cdots O} = 2.89$ Å, evaluated from various organic crystals.[57] On the other hand, presence of hydrogen bonds between urea–water and urea–urea molecules are suggested from the present intermolecular N–N and N–H partial structure functions as mentioned above. It is considered that the first peak in the present $g_{NO(NC)}^{inter}(r)$ involves contributions from hydrogen-bonded N···O(water), N···O(urea) interactions and non-bonded ones between N and O atom. In the least-squares fitting analysis of the observed $a_{NO(NC)}^{inter}(Q)$ function, contributions from both hydrogen-bonded and non-bonded N···O interactions were both involved in the model function. Non-bonded N···C interaction was added to the model function in order to take into account for the short-range N···C interaction within the urea dimer, which is expected at ca. 4 Å for both head-to-tail and cyclic configurations.

Final results of the least-squares fitting refinement are summarized in Table 3. The present value of the nearest neighbor N···O distance, $r_{NO} = 3.14(1)$ Å, is ca. 0.2 Å longer than that reported for aqueous 15 mol % urea solution ($r_{NO} =$ 2.92 Å),[7] suggesting that the nearest neighbor N···O(water) interaction is considerably perturbed by the urea aggregation. The nearest neighbor N···C distance was determined to be $r_{NC} = 4.09(3)$ Å, which is consistent with that expected for the N···C distance within urea dimer. These results clearly indicate that self-aggregation of urea molecules occurs in the present solution. The hydrogen-bonded structure among solvent water molecules is investigated through the analysis of the H–H, X–H, and X–X partial structure functions, which is described in the following section.

H–H, X–H, and X–X Partial Structure Functions. In order to obtain direct structural information concerning the intermolecular hydrogen-bonded interaction in highly concentrated aqueous urea solution, neutron diffraction measurements of H/D isotopically substituted aqueous 25 mol % urea solutions were carried out. At least three independent diffraction data sets from sample solutions with different H/D ratios are necessary to derive partial structure factors, $a_{HH}(Q)$, $a_{XH}(Q)$, and $a_{XX}(Q)$ (X: O, C, and N).[58–65] In the present study, values of the mole fraction of deuterium atom, f_D, in samples were chosen to be $f_D = 0.999$, 0.697, and 0.359. In the third sample, the average coherent scattering length of hydrogen atom was set to be zero, which implies that interference term observed for this solution can directly be connected to the X–X partial structure function as indicated in eq 20. The f_D value for the second sample was chosen in order to avoid larger incoherent scattering from the H nucleus and to maintain favorable conditions for solving the simultaneous equations to derive the $a_{HH}(Q)$ and $a_{XH}(Q)$.

The scattering cross section observed for aqueous 25 mol % urea solutions with different H/D isotopic ratios is shown in Figure 8. As mentioned in the former section, the inelasticity contribution involved in the self term can be sufficiently cancelled out in the first-order difference function, $\Delta_N(Q)$, however contribution from the inelasticity effect should remain in the case of the difference function between H/D substituted samples. Therefore, we have to evaluate the self term involved in observed scattering cross section for samples VI, VII, and VIII to derive H–H, X–H, and X–X partial structure factors. In principle, the inelasticity effect caused from H atom is expected to cancel out in obtaining the H–H partial structure factor by eq 18. However, the multiple scattering contribution should be involved in the present cross sections for these samples, which makes direct evaluation of the $a_{HH}(Q)$ from the combination of observed $(d\sigma/d\Omega)^{obs}$ difficult. Therefore, we obtained the intermolecular interference term, $(d\sigma/d\Omega)^{inter}$, by means of the least-squares fitting procedure in which the self term was described as a polynomial expansion of Q (eq 5). Calculated self term of each sample solution is depicted by the broken line in Figure 8. The intensity of calculated self term monotonically decreases with increasing Q value and does not introduce any oscillation which might affect the extraction of the interference term. The sum of contributions from the calculated self term and intramolecular interference term in eq 2 (shown by the solid line) was then subtracted from the observed $(d\sigma/d\Omega)^{obs}$ to obtain the intermolecular interference term, $(d\sigma/d\Omega)^{inter}$, which is shown in Figure 9.

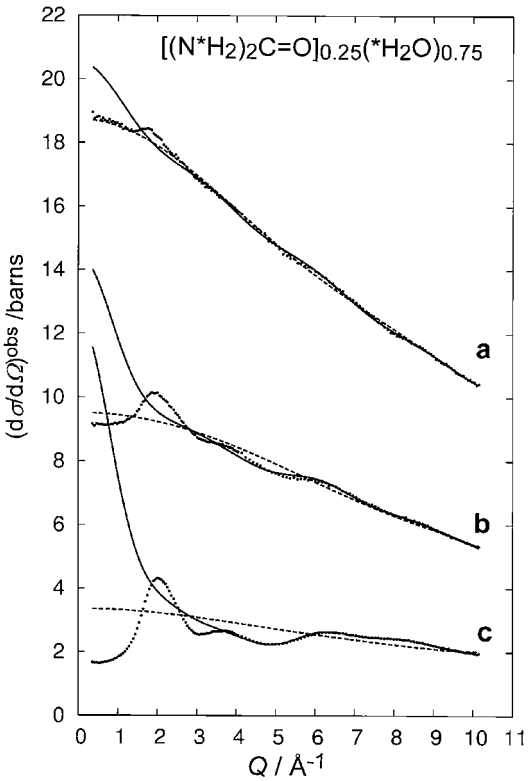

Figure 8. Scattering cross section, $(d\sigma/d\Omega)^{obs}$, observed for sample solutions (a) VII, (b) VIII, and (c) VI (dots). The self scattering intensity is denoted by the broken line. Sum of contributions from the intramolecular interference and the self scattering terms is shown by the solid line.

The $(d\sigma/d\Omega)^{inter}$ terms preferably oscillate around zero, indicating that the present procedure for extracting the intermolecular interference contribution from the observed scattering cross section works successfully. Difference in the oscillational amplitude between these samples is due to the difference in the average coherent scattering length of the hydrogen atom. Observed interference term for ^{0}H involves no contribution from H–H, O–H, N–H, and C–H correlations. Prior to deriving partial structure factor, correction for the low-frequency systematic errors was applied to the observed $(d\sigma/d\Omega)^{inter}$.[46]

Three intermolecular partial structure factors, $a_{HH}^{inter}(Q)$, $a_{XH}^{inter}(Q)$, and $a_{XX}^{inter}(Q)$, were derived from the combination of the observed $(d\sigma/d\Omega)^{inter}$ terms using eqs 18–20. These partial structure factors are shown in Figure 10. Corresponding intermolecular partial pair correlation functions are given in Figure 11. The first peak in the present $g_{HH}^{inter}(r)$ is considerably smeared when compared with that reported for liquid pure water,[58,59] indicating that hydrogen bonds between neighboring water molecules are very weak in the highly concentrated aqueous urea solution. A small first peak appearing at $r \approx 2$ Å in the present $g_{XH}^{inter}(r)$ is attributable to the nearest neighbor O···H interaction between water molecules. The area under this peak is much smaller than that found in pure liquid water,[58,59] in which water molecules form a

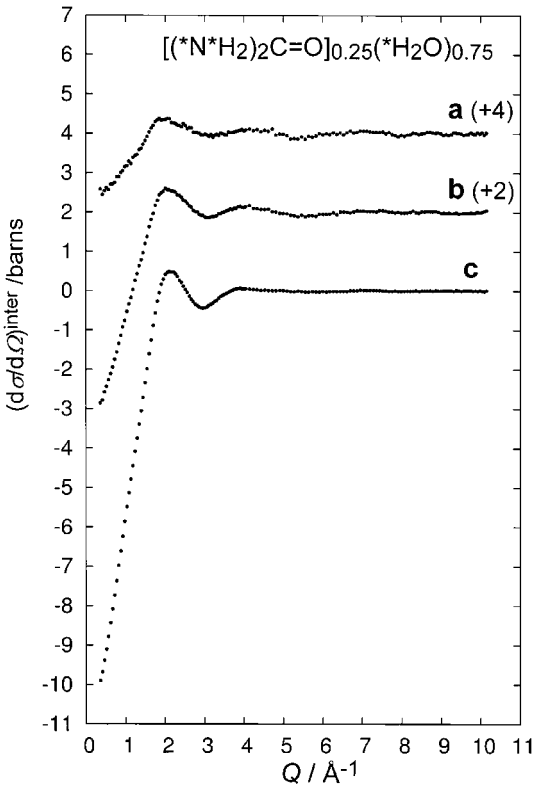

Figure 9. Intermolecular interference term, $(d\sigma/d\Omega)^{inter}$, observed for (a) sample VII, (b) VIII, and (c) VI (dots).

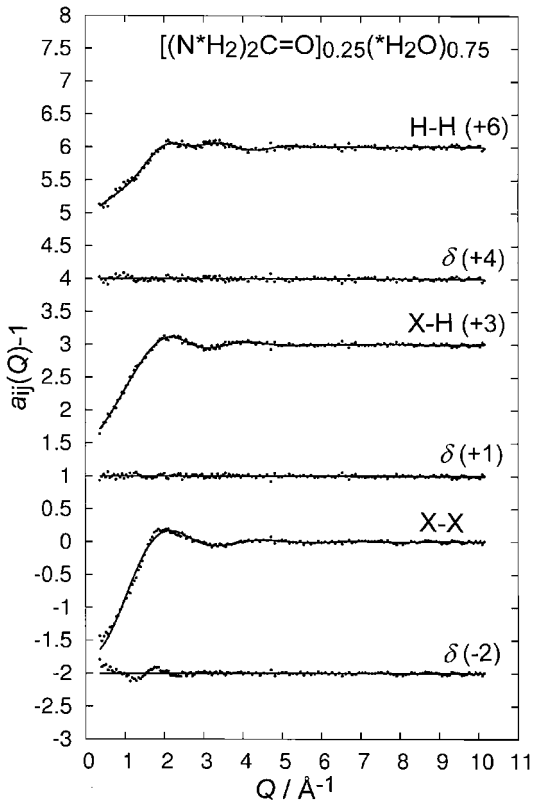

Figure 10. Intermolecular (a) H–H, (b) X–H, and (c) X–X partial structure factors (X: O, C, and N) (dots). The best-fit of calculated interference term (solid line). The difference between observed and calculated interference function is given below.

tetrahedral hydrogen-bonded network. In the present concentrated urea solution, this hydrogen-bonded network is considerably modified. The same conclusion can be drawn from the present $g_{XX}^{inter}(r)$, in which distinct hydrogen-bonded O···O peak at $r \approx 2.8$ Å is absent, which is in contrast to the well-defined nearest neighbor O···O peak appearing in $g_{OO}(r)$ for pure water,[29] applying smaller Q_{max} (=9.8 Å^{-1}) in the Fourier transform than that employed in the present work. This implies that the broadened feature of the present $g_{XX}(r)$ cannot be related to the relatively smaller value of Q_{max}. The nearest neighbor hydrogen-bonded interaction between water molecules in the present solution is considerably different from that in liquid pure water.

Structural parameters, r_{ij}, l_{ij}, and n_{ij}, were determined by the least-squares fit to observed $a_{ij}^{inter}(Q)$ using the model interference function in eq 22, involving short- and long-range contributions. In the fitting procedure of $a_{HH}^{inter}(Q)$, at least three short-range interactions were found to be necessary to reproduce the observed $a_{HH}^{inter}(Q)$. Then, the refinement was carried out assuming that three short-range interactions and a long-range contribution are involved in the model function. The model function employed in the analysis of the present $a_{XH}^{inter}(Q)$ involves two short-range O···H interactions, two short-range N···H interactions and a long-range contribution. In the fitting procedure, structural parameters for the N···H interactions were fixed at values that have already been determined from the least-squares analysis of the observed $a_{NH}^{inter}(Q)$. In the fitting of the observed $a_{XX}^{inter}(Q)$, parameters for two short-range O···O interactions and long-range contribution were refined independently. Short-range contributions from N···O and N···C interactions were involved in the model function. Parameters for these interactions were fixed at values determined from the analysis of the observed $a_{NO(NC)}^{inter}(Q)$ as described above.

Results of the least-squares refinements are summarized in Table 4. The present value of the nearest neighbor H···H distance, $r_{HH} = 2.37(5)$ Å is in good agreement with that reported for liquid pure water (2.4 Å).[29,64] On the other hand, the coordination number for the intermolecular nearest neighbor H···H interaction ($n_{HH} = 2.0(5)$), is much smaller than that for pure water ($n_{HH} = 4.0$),[65] which implies that intermolecular hydrogen bonds among water molecules are significantly broken in the present solution. The second nearest neighbor H···H distance is determined to be $r_{HH} = 2.90(5)$ Å, which seems too long for the hydrogen-bonded interaction. The longer nearest neighbor H···H distance, $r_{HH} = 2.53$ Å, has been found in aqueous 15.3 mol % urea solution,[11] in which contributions from H_W–H_W, H_U–H_W, and H_U–H_U (H_W: water hydrogen, H_U: urea hydrogen) pairs are estimated to be 54%, 39%, and 7%, respectively. The present $a_{HH}^{inter}(Q)$ (and $g_{HH}^{inter}(r)$) contains contribution from water–water (16%) urea–water (48%), and urea–urea (16%) interactions. According to the Monte Carlo simulation study by Hernández-Cobos et al., the position of the lower-r shoulder of the broadened nearest neighbor interaction is located at $r = 2.8$–2.9 Å for the H_U–H_W and H_U–H_U partial pair correlation functions.[66] The

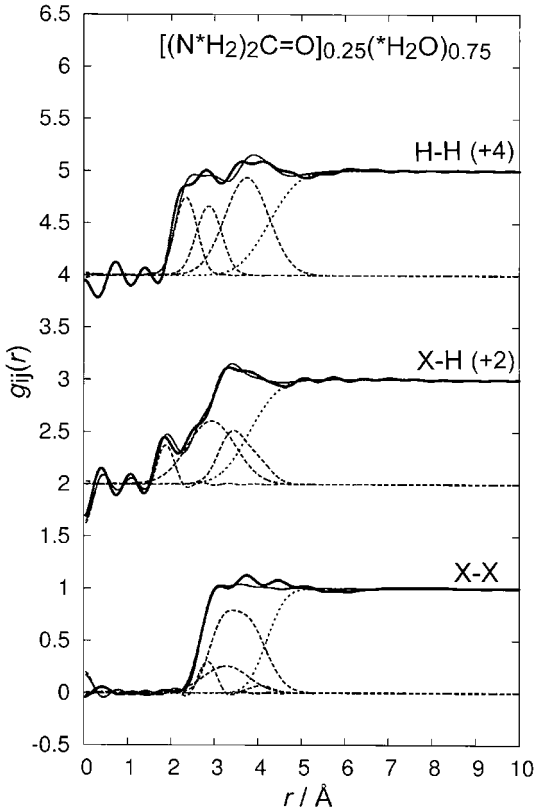

Figure 11. Intermolecular (a) H–H, (b) X–H, and (c) X–X partial pair correlation functions observed for aqueous 25 mol % urea solutions (thick solid line). Fourier transform of the best-fit of calculated interference terms shown in Figure 10 (thin solid line). Broken and dotted lines show short- and long-range components, respectively.

small value of n_{HH} for the first peak of the present $g_{HH}^{inter}(r)$ indicates that the hydrogen-bonded networks among water molecules are significantly affected by the H_U–H_W and H_U–H_U interactions.

The present value of the nearest neighbor O···H peak position, $r_{OH} = 1.90(1)$ Å, is slightly larger than that reported for liquid pure water (1.85 Å),[29,58] while it is in good agreement with those observed for 8 mol % NH_4Cl ($r_{OH} = 1.91$ Å),[60] 10 mol % LiBr ($r_{OH} = 1.91$ Å),[61] and 2.5 mol % alanine ($r_{OH} = 1.90$ Å)[62] aqueous solutions. The present nearest neighbor O···H coordination number ($n_{OH} = 0.83$) is considerably smaller than that reported for liquid pure water, $n_{OH} = 1.8$–2.2.[29,67–69] The result again indicates that the hydrogen bonds among water molecules are significantly broken in the concentrated urea solution.

The present value of the nearest neighbor O···O distance, $r_{OO} = 2.86(2)$ Å, agrees well with that reported for liquid pure water ($r_{OO} = 2.88$ Å[29] and 2.78–2.82 Å[69]), implying that the hydrogen bonds between water molecules remain in the present solution. On the other hand, the remarkably small value of the n_{OO} (=1.4(1)) confirms the breakdown of the tetrahedral network of water molecules. The second nearest neighbor O···O peak located at $r_{OO} = 3.35(6)$ Å is attributable to the weakly interacting water–water correlation.[53,70] The present nearest neighbor O···O peak should involve contribution from O_W–O_W (56%), O_U–O_W (38%), and O_U–O_U (6%) interactions. It is supposed that an overlap of these contributions may result in the broadened shape of the present $g_{XX}^{inter}(r)$.

Table 4. Results of the Least-Squares Refinement for Intermolecular Partial Structure Factors, $a_{HH}^{inter}(Q)$, $a_{XH}^{inter}(Q)$, and $a_{XX}^{inter}(Q)$, Observed for Aqueous 25 mol % Urea Solutions[a)]

		$a_{HH}^{inter}(Q)-1$	$a_{XH}^{inter}(Q)-1$	$a_{XX}^{inter}(Q)-1$
Short-range	i–j	H–H	O–H	O–O
	r_{ij}/Å	2.37(5)	1.90(1)	2.86(2)
	l_{ij}/Å	0.25(5)	0.12(1)	0.15(1)
	n_{ij}	2.0(5)	0.83(1)	1.4(1)
	i–j	H–H	O–H	O–O
	r_{ij}/Å	2.90(5)	3.04(1)	3.35(6)
	l_{ij}/Å	0.29(1)	0.54(1)	0.51(1)
	n_{ij}	3.1(5)	11.8(1)	4.8(3)
	i–j	H–H	N–H	N–O
	r_{ij}/Å	3.81(2)	3.42(fixed)	3.14(fixed)
	l_{ij}/Å	0.50(2)	0.31(fixed)	0.28(fixed)
	n_{ij}	12.8(3)	8.3(fixed)	2.2(fixed)
	i–j	—	N–H	N–O
	r_{ij}/Å	—	4.01(fixed)	3.77(fixed)
	l_{ij}/Å	—	0.31(fixed)	0.45(fixed)
	n_{ij}	—	5.2(fixed)	9.3(fixed)
				N–C
				4.09(fixed)
				0.26(fixed)
				1.1(fixed)
Long-range	r_0/Å	4.31(4)	3.88(1)	4.23(1)
	l_0/Å	0.53(1)	0.52(1)	0.34(1)

a) Estimated errors are given in parentheses.

The present results clearly indicate that hydrogen bonds among the nearest neighbor water molecules in highly concentrated urea solutions are considerably broken compared to those in pure water. This implies that the environment of the surface of the protein can be more hydrophobic in highly concentrated urea solutions, which may help denature the protein.

Conclusion

In conclusion, partial pair correlation functions directly derived from neutron diffraction data clearly indicate the aggregation of urea molecules in the aqueous 25 mol % urea solution. Experimental evidence of the extensive breakdown of hydrogen-bonded network structure of water molecules has been obtained from partial structure functions directly obtained from the observed scattering cross sections for isotopically substituted samples. The present results on the formation of urea oligomers and extensive breakdown of hydrogen bonds among water molecules are thought to strongly relate to the molecular mechanism of protein denaturation by concentrated aqueous urea solutions.

The authors thank the Institute of Solid State Physics (ISSP), the University of Tokyo, for allowing us to use the 4G

(GPTAS) diffractometer. We are grateful to Prof. Taku J. Sato (ISSP, the University of Tokyo) for his help during the course of neutron diffraction measurements. We acknowledge Prof. Hideki Yoshizawa (ISSP, the University of Tokyo) and Mr. Yoshihisa Kawamura (ISSP, the University of Tokyo) for their stimulating discussions and encouragement. All calculations were carried out the Yamagata University Networking and Computing Center. This work was partially supported by Grant-in-Aid for Scientific Research (C) (No. 20550055), from the Ministry of Education, Culture, Sports, Science and Technology, Japan.

References

1 J. L. Finney, J. Turner, *Ann. N.Y. Acad. Sci.* **1986**, *482*, 127.
2 J. Turner, J. L. Finney, J. P. Bouquiere, G. W. Neilson, S. Cummings, J. Bouillot, *Physica B+C* **1986**, *136*, 260.
3 J. Turner, J. L. Finney, J. P. Bouquiere, G. W. Neilson, S. Cummings, J. Bouillot, in *Water and Aqueous Solutions*, ed. by G. W. Neilson, J. E. Enderby, Adam Hilger, Bristol and London, **1986**, p. 277.
4 J. L. Finney, J. Turner, *Electrochim. Acta* **1988**, *33*, 1183.
5 J. Turner, J. L. Finney, A. K. Soper, *Z. Naturforsch., A: Phys. Sci.* **1991**, *46*, 73.
6 J. L. Finney, A. K. Soper, *Chem. Soc. Rev.* **1994**, *23*, 1.
7 Y. Kameda, H. Naganuma, K. Mochiduki, M. Imano, T. Usuki, O. Uemura, *Bull. Chem. Soc. Jpn.* **2002**, *75*, 2579.
8 A. K. Soper, E. W. Castner, Jr., A. Luzar, *Biophys. Chem.* **2003**, *105*, 649.
9 R. C. Burton, E. E. Ferrari, R. J. Davey, J. Hopwood, M. J. Quayle, J. L. Finney, D. T. Bowron, *Cryst. Growth Des.* **2008**, *8*, 1559.
10 Y. Kameda, M. Sasaki, S. Hino, Y. Amo, T. Usuki, *Bull. Chem. Soc. Jpn.* **2006**, *79*, 1367.
11 J. L. Finney, A. K. Soper, J. Turner, *Physica B* **1989**, *156–157*, 151.
12 R. Adams, H. H. M. Balyuzi, R. E. Burge, *J. Appl. Crystallogr.* **1977**, *10*, 256.
13 P.-O. Åstrand, A. Wallqvist, G. Karlström, *J. Phys. Chem.* **1994**, *98*, 8224.
14 A. Idrissi, F. Sokolić, A. Perera, *J. Chem. Phys.* **2000**, *112*, 9479.
15 B. Kallies, *Phys. Chem. Chem. Phys.* **2002**, *4*, 86.
16 F. Sokolić, A. Idrissi, A. Perera, *J. Chem. Phys.* **2002**, *116*, 1636.
17 F. Sokolić, A. Idrissi, A. Perera, *J. Mol. Liq.* **2002**, *101*, 81.
18 S. Weerasinghe, P. E. Smith, *J. Phys. Chem. B* **2003**, *107*, 3891.
19 A. Idrissi, E. Cinar, S. Longelin, P. Damay, *J. Mol. Liq.* **2004**, *110*, 201.
20 V. F. Sears, *Neutron News* **1992**, *3*, 26.
21 J. G. Powles, *Adv. Phys.* **1973**, *22*, 1.
22 J. R. Granada, V. H. Gillete, R. E. Mayer, *Phys. Rev. A* **1987**, *36*, 5594.
23 H. H. Paalman, C. J. Pings, *J. Appl. Phys.* **1962**, *33*, 2635.
24 Y. Kameda, H. Ebata, T. Usuki, O. Uemura, M. Misawa, *Bull. Chem. Soc. Jpn.* **1994**, *67*, 3159.
25 Y. Kameda, T. Mori, T. Nishiyama, T. Usuki, O. Uemura, *Bull. Chem. Soc. Jpn.* **1996**, *69*, 1495.
26 Y. Kameda, K. Sugawara, T. Hosaka, T. Usuki, O. Uemura, *Bull. Chem. Soc. Jpn.* **2000**, *73*, 1105.
27 Y. Kameda, K. Sugawara, T. Usuki, O. Uemura, *Bull. Chem. Soc. Jpn.* **2003**, *76*, 935.
28 Y. Kameda, M. Sasaki, Y. Amo, T. Usuki, *Bull. Chem. Soc. Jpn.* **2006**, *79*, 228.
29 A. K. Soper, M. G. Phillips, *Chem. Phys.* **1986**, *107*, 47.
30 J. Dawidowski, J. R. Granada, R. E. Mayer, G. J. Cuello, V. H. Gillette, M.-C. Bellissent-Funel, *Physica B* **1994**, *203*, 116.
31 I. A. Blech, B. L. Averbach, *Phys. Rev.* **1965**, *137*, A1113.
32 H. Bertagnolli, P. Chieux, H. G. Hertz, *Ber. Bunsen-Ges. Phys. Chem.* **1984**, *88*, 977.
33 G. Placzek, *Phys. Rev.* **1952**, *86*, 377.
34 J. G. Powles, *Mol. Phys.* **1979**, *37*, 623.
35 M. Rovere, L. Blum, A. H. Narten, *J. Chem. Phys.* **1980**, *73*, 3729.
36 J. G. Powles, *Mol. Phys.* **1981**, *42*, 757.
37 J. R. Granada, *Phys. Rev. B* **1985**, *31*, 4167.
38 D. G. Montague, I. P. Gibson, J. C. Dore, *Mol. Phys.* **1981**, *44*, 1355.
39 D. G. Montague, J. C. Dore, *Mol. Phys.* **1986**, *57*, 1035.
40 D. G. Montague, I. P. Gibson, J. C. Dore, *Mol. Phys.* **1982**, *47*, 1405.
41 D. C. Champeney, R. N. Joarder, J. C. Dore, *Mol. Phys.* **1986**, *58*, 337.
42 M.-C. Bellissent-Funel, L. Bosio, J. Teixeira, *J. Phys.: Condens. Matter* **1991**, *3*, 4065.
43 S. Swaminathan, B. M. Craven, *Acta Crystallogr., Sect. B* **1984**, *40*, 300.
44 K. Iijima, K. Tanaka, S. Onuma, *J. Mol. Struct.* **1991**, *246*, 257.
45 C. Kato, S. Konaka, T. Iijima, M. Kimura, *Bull. Chem. Soc. Jpn.* **1969**, *42*, 2148.
46 Y. Kameda, O. Uemura, *Bull. Chem. Soc. Jpn.* **1992**, *65*, 2021.
47 J. C. Dore, M. Garawi, M.-C. Bellissent-Funel, *Mol. Phys.* **2004**, *102*, 2015.
48 T. Nakagawa, Y. Oyanagi, *Recent Developments in Statistical Inference and Data Analysis*, North-Holland, Amsterdam, **1980**, p. 221.
49 A. K. Soper, G. W. Neilson, J. E. Enderby, R. A. Howe, *J. Phys. C: Solid State Phys.* **1977**, *10*, 1793.
50 J. E. Enderby, G. W. Neilson, in *Water: A Comprehensive Treatise*, ed. by F. Franks, Plenum Press, New York, **1979**, Vol. 6, p. 1.
51 J. E. Enderby, *Chem. Soc. Rev.* **1995**, *24*, 159.
52 G. W. Neilson, J. E. Enderby, *Proc. R. Soc. London, Ser. A* **1983**, *390*, 353.
53 A. H. Narten, M. D. Danford, H. A. Levy, *Discuss. Faraday Soc.* **1967**, *43*, 97.
54 R. Caminiti, P. Cucca, M. Monduzzi, G. Saba, G. Crisponi, *J. Chem. Phys.* **1984**, *81*, 543.
55 H. Ohtaki, N. Fukushima, *J. Solution Chem.* **1992**, *21*, 23.
56 A. Caballero-Herrera, L. Nilsson, *THEOCHEM* **2006**, *758*, 139.
57 L. N. Kuleshova, P. Zorkii, *Acta Crystallogr., Sect. B* **1981**, *37*, 1363.
58 A. K. Soper, F. Bruni, M. A. Ricci, *J. Chem. Phys.* **1997**, *106*, 247.
59 A. K. Soper, *Chem. Phys.* **2000**, *258*, 121.
60 Y. Kameda, K. Sugawara, T. Usuki, O. Uemura, *J. Phys. Soc. Jpn.* **2001**, *70*, Suppl. A, 362.
61 Y. Kameda, M. Imano, M. Takeuchi, S. Suzuki, T. Usuki, O. Uemura, *J. Non-Cryst. Solids* **2001**, *293–295*, 600.
62 Y. Kameda, M. Sasaki, M. Yaegashi, Y. Amo, T. Usuki,

Bull. Chem. Soc. Jpn. **2004**, *77*, 1807.
63 Y. Kameda, K. Yamanaka, M. Sasaki, Y. Amo, T. Usuki, *Bull. Chem. Soc. Jpn.* **2006**, *79*, 1032.
64 Y. Kameda, T. Usuki, O. Uemura, *Bull. Chem. Soc. Jpn.* **1998**, *71*, 1305.
65 T. Otomo, H. Iwase, Y. Kameda, N. Matubayasi, K. Itoh, S. Ikeda, M. Nakahara, *J. Phys. Chem. B* **2008**, *112*, 4687.
66 J. Hernández-Cobos, I. Ortega-Blake, M. Bonilla-Marín, M. Moreno-Bello, *J. Chem. Phys.* **1993**, *99*, 9122.
67 P. Postorino, M. A. Ricci, A. K. Soper, *J. Chem. Phys.* **1994**, *101*, 4123.
68 A. K. Soper, *Chem. Phys.* **1984**, *88*, 187.
69 A. K. Soper, *J. Phys.: Condens. Matter* **2007**, *19*, 335206.
70 K. Yamanaka, T. Yamaguchi, H. Wakita, *J. Chem. Phys.* **1994**, *101*, 9830.